

# End-to-End Entanglement Rate: Toward a Quantum Route Metric

Marcello Caleffi\*<sup>†</sup>, *Senior Member, IEEE*

\* Dept. of Electrical Engineering and Information Technologies (DIETI)

University of Naples Federico II, Naples, Italy

Email: marcello.caleffi@unina.it

<sup>†</sup> National Laboratory of Multimedia Communication

National Inter-University Consortium for Telecommunications (CNIT), Naples, Italy

**Abstract**—We present an entanglement-generation rate analysis for generic quantum network architectures composed by repeaters operating through single atoms in optical cavities. Specifically, we analytically derive the *end-to-end entanglement rate* between a couple of nodes through an arbitrary path. To this aim, we first model the entanglement generation through a stochastic framework that allows us to jointly account for all the key physical-mechanisms affecting the end-to-end entanglement rate, such as decoherence time, atom-photon and photon-photon entanglement generation, entanglement swapping and imperfect bell-state measurement. Then, we derive the closed-form expression of the *end-to-end entanglement rate*. Finally, we evaluate the entanglement rate under realistic parameter setting.

**Index Terms**—Quantum Networks; Quantum Routing; Quantum Repeater; Entanglement Rate; Route; Path; Metric.

## I. INTRODUCTION

Despite the tremendous progress of quantum technologies, long-distance efficient entanglement distribution still constitutes a key issue, due to the exponential decay of communication rate as a function of the distance [1], [2]. A viable solution to significantly improve the entanglement distribution rate over long distances is the adoption of *quantum repeaters* [3], [4]. As shown in Figure 1, instead of distributing entanglement over a long link, entanglement will be generated through smaller links. A combination of *entanglement swapping* [5] and *entanglement purification* [6] performed at each quantum repeater enables one to extend the entanglement over the entire channel. Independently from the presence of quantum repeaters, another key issue for efficient entanglement distribution is constituted by the *quantum decoherence*, which involves a loss of the entanglement between the entangled entities as time passes, as shown in Figure 1.

Hence, in this paper, we analytically derive the *end-to-end entanglement rate* through an arbitrary path in a quantum network. To this aim, we model the entanglement generation through a stochastic framework. As opposed to existing literature [7]–[11], we jointly account for all the key physical-mechanisms affecting the end-to-end entanglement rate, such as decoherence time, atom-photon and photon-photon entanglement generation, entanglement swapping and imperfect bell-state measurement. Furthermore, differently from the existing literature, we derive a closed-form expression of the entanglement rate for an arbitrary path, by relaxing the

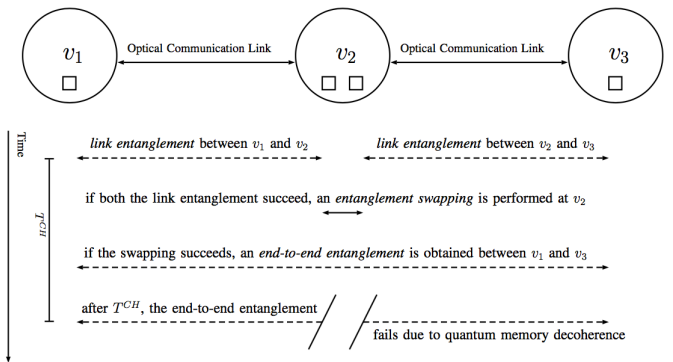


Fig. 1. Schematic illustration of the end-to-end entanglement generation between nodes  $v_1$  and  $v_3$  through quantum repeater  $v_2$ , with quantum memories depicted as squares and  $T^{CH}$  denoting the decoherence time. Time duration proportion among operations not respected for the sake of clarity.

constraint that repeaters must split the long-range link into segments of equal length. This is a valuable property, since it allows our rate expression to be used as routing metric by an arbitrary quantum routing protocol.

The rest of the paper is organized as follows. In Sec. II, we describe the network model along with some preliminaries. In Sec. III, we analytically derive the closed-form expression of the *end-to-end entanglement rate*, whereas in Sec. IV we evaluate the rate under realistic parameter setting. In Sec. V, we conclude the paper, and, finally, some proofs are gathered in the Appendix.

## II. QUANTUM NETWORK ARCHITECTURE

We consider a quantum network architecture where the heralding detection of an entanglement generation is based on single-photon detection, and high-fidelity entangled pairs are created at the price of low entanglement generation success probabilities [11]–[15].

Specifically, as shown in Figure 2, a quantum repeater consists of an atom storing a qubit and surrounded by two cavities: an *heralding cavity* and a *telecom-wavelength entangling cavity*. The atoms ( $^{87}\text{Rb}$  rubidium isotopes) are individually excited by laser pulses, which allow the heralded entanglement

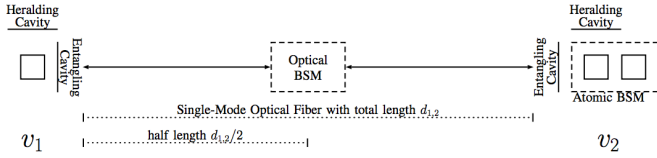


Fig. 2. Schematic illustration of a quantum repeater operating through single atoms in optical cavities. Dimension proportion among different components not respected for the sake of clarity.

between the atom and a telecom-wavelength photon<sup>1</sup>. More in detail, the heralding cavity is responsible for detecting the entanglement generation, whereas the entangling cavity is responsible for coupling the telecom-wavelength photon to the mode of single-mode optical telecom fiber.

Once an atom-photon entanglement is locally generated at each node, a remote entanglement between two adjacent nodes<sup>2</sup> is generated by entanglement swapping through *optical Bell-State Measurement (BSM)* of the two photons.

Finally, remote entanglement between non-adjacent nodes is generated by performing entanglement swapping at intermediate nodes through an *atomic BSM* between the atom pair stored at each intermediate node. Specifically, cavity-assisted quantum gate is performed on two atoms via reflection of a single photon originating from a cavity-based single-photon source (SPS). Subsequent detection of the atomic quantum states in suitable bases allows for an unambiguous determination of the two-particle Bell state. This results in an entangled state between the two non-adjacent nodes.

In the following, we denote the quantum network with the graph  $G = (V, E)$ , with  $V = \{v_i\}_{i=1}^N$  and  $E = \{e_{i,j}, v_i, v_j \in V\}$  denoting the set of nodes and optical links, respectively.

Given an arbitrary couple of nodes  $v_i$  and  $v_j$ , if it exists  $e_{i,j} \in E$  then  $v_i$  and  $v_j$  are defined *adjacent* nodes.  $d_{i,j}$  and  $\tau_{i,j}^c$  denote the length of the optical link and the average time<sup>3</sup> required for a classical communication between node  $v_i$  and  $v_j$ , respectively.

The route  $\mathcal{R}_{i,j}$  denotes a simple path between two arbitrary nodes  $v_i$  and  $v_j$ , i.e., a finite ordered sequence of edges  $(e_{\sigma_1, \sigma_2}, \dots, e_{\sigma_{n-1}, \sigma_n})$  in  $E$  so that  $v_{\sigma_1} = v_i$ ,  $v_{\sigma_n} = v_j$ , and  $\sigma_i \neq \sigma_j$  for any  $i, j$ .  $T_{\mathcal{R}_{i,j}}^c = \sum_{i=1}^{n-1} \tau_{\sigma_i, \sigma_{i+1}}^c$  denotes the average time required for a classical communication between nodes  $v_i$  and  $v_j$  through path  $\mathcal{R}_{i,j}$ .

**Definition 1. (Local Entanglement Probability)** The *local entanglement generation probability*  $p_i$  denotes the probability of successfully generating an atom-photon entanglement at node  $v_i \in V$ .

**Definition 2. (Local Entanglement Time)** The *local entanglement generation time*  $T_i$  denotes the average time required

<sup>1</sup>I.e., a photon with a wavelength assuring low absorption in optical telecom single-mode fibers, hence, facilitating long-distance communications.

<sup>2</sup>I.e., two quantum repeaters connected by an optical fiber.

<sup>3</sup>In the following, we assume without loss of generality  $\tau_{i,j}^c = \tau_{j,i}^c$ .

for successfully generating an atom-photon entanglement at node  $v_i \in V$ .

**Definition 3. (Link Entanglement Probability)** The *link entanglement generation probability*  $p_{i,j}$  denotes the probability of successfully generating a remote entanglement between two adjacent nodes  $v_i$  and  $v_j$  through optical link  $e_{i,j}$ .

**Definition 4. (Link Entanglement Time)** The *link entanglement generation time*  $T_{i,j}$  denotes the average time required for successfully generating a remote entanglement between two adjacent nodes  $v_i$  and  $v_j$  through optical link  $e_{i,j}$ .

**Definition 5. (End-to-End Entanglement Probability)** The *end-to-end entanglement generation probability*  $p_{\mathcal{R}_{i,j}}$  denotes the probability of successfully generating a remote entanglement between two nodes  $v_i$  and  $v_j$  through route  $\mathcal{R}_{i,j}$ .

**Definition 6. (End-to-End Entanglement Time)** The *end-to-end entanglement generation time*  $T_{\mathcal{R}_{i,j}}$  denotes the average time required for successfully generating a remote entanglement between two nodes  $v_i$  and  $v_j$  through route  $\mathcal{R}_{i,j}$ .

### III. END-TO-END ENTANGLEMENT RATE

Here, we first analytically derive in Sec. III-A the closed-form expression of the expected link entanglement generation rate. Then, we analytically derive in Sec. III-B the closed-form expression of the expected end-to-end entanglement generation rate. Finally, we discuss the derived results in Section III-C.

#### A. Link Entanglement

First, we observe that the local entanglement generation probability  $p_i$  at node  $i$  is affected by two main factors [11]:

- i) successful generation of a herald photon and a telecom photon, assumed constant at each node since influenced by the isotope unwanted initial-states and decay-paths;
- ii) the parasitic losses in the heralding and entangling cavity, assumed constant at each node since influenced by the detector technology.

Hence,  $p_i$  can be written as:

$$p = p_i = (p^{ht} \nu^h \nu^t) \quad \forall v_i \in V \quad (1)$$

with  $p^{ht}$  denoting the photons generation probability, and  $\nu^h$  and  $\nu^t$  denoting the heralding and entangling detector efficiency, respectively.

Once a heralded local entanglement is generated at each node, the two photons must be sent to the BSM and must be measured. Hence, by accounting for (1), the link entanglement generation probability  $p_{i,j}$  is equal to [11]:

$$p_{i,j} = \frac{1}{2} \nu^o \left( p e^{-d_{i,j}/(2L_0)} \right)^2 = \frac{1}{2} \nu^o p^2 e^{-d_{i,j}/L_0} \quad (2)$$

where  $\nu^o$  denotes the optical BSM efficiency (assumed constant at each node),  $d_{i,j}$  denotes the length of link  $e_{i,j}$ ,  $L_0$  denotes the attenuation length of the optical fiber, and the term

$\frac{1}{2}$  accounts for the optical BSM capability of unambiguously identifying only two out of four bell states.

The average time  $T_i$  required for a single atom-photon entanglement operation is equal to:

$$T = T_i = \tau^p + \max\{\tau^h, \tau^t\} \forall v_i \in V \quad (3)$$

with  $\tau^p$  denoting the duration of the pulse required to excite the atom, and  $\tau^h$  and  $\tau^t$  denoting the time expectation for heralding-cavity and telecom-cavity output (again, assumed constant at each node without loss of generality).

Once an atom-photon entanglement operation is performed, the two photons must be sent to the optical BSM, and then an acknowledgment of the arrival of the photons must be sent back from the BSM to each node<sup>4</sup>. If the first link entanglement attempt succeeds, the average time  $T_{i,j}^s$  required for the successful attempt is equal to:

$$T_{i,j}^s = \tau^p + \max\{\tau^h, \tau_{i,j}\} \quad (4)$$

where

$$\tau_{i,j} = \tau^t + \tau^o + \tau_{i,j}^c + \frac{d_{i,j}}{2c_f} \quad (5)$$

with  $\tau^o$  denoting the time required for the optical BSM,  $\tau_{i,j}^c$  denoting the time required for ack transmission over classical communication link between nodes  $v_i$  and  $v_j$ , and  $c_f$  denoting the light speed in optical fiber. Otherwise, if the first attempt fails, an additional time  $\tau^d$  is required for cooling the atom before to start a new local entanglement generation, and the total average time  $T_{i,j}^f$  required for the failed attempt is equal to:

$$T_{i,j}^f = \tau^p + \max\{\tau^h, \tau_{i,j}, \tau^d\} \quad (6)$$

By accounting for (2) and (6), we derive in Lemma 1 the average time  $T_{i,j}$  for a link entanglement generation

**Lemma 1. (Link Entanglement Generation Time)** *The average time required to generate a remote entanglement between two adjacent nodes  $v_i$  and  $v_j$  is equal to:*

$$T_{i,j} = \frac{\bar{p}_{i,j} T_{i,j}^f + p_{i,j} T_{i,j}^s}{p_{i,j}} \quad (7)$$

with  $\bar{p}_{i,j} \triangleq 1 - p_{i,j}$  and  $T_{i,j}^f$  and  $T_{i,j}^s$  given in (4) and (6), respectively.

*Proof: See Appendix A.* ■

From Lemma 1, the main result follows.

**Theorem 1. (Link Entanglement Generation Rate)** *The expected entanglement generation rate  $R_{i,j}(T^{ch})$  between adjacent nodes  $v_i$  and  $v_j$  is equal to:*

$$R_{i,j}(T^{ch}) = \begin{cases} 0 & \text{if } T^{ch} < \tau_{i,j} \\ 1/T_{i,j} & \text{otherwise} \end{cases} \quad (8)$$

with  $T^{ch}$  denoting the quantum memory coherence time and  $\tau_{i,j}$  given in (5).

*Proof: See Appendix B.* ■

<sup>4</sup>The acks can be sent through full-duplex optical links with classical communications characterized by a negligible error rate.

## B. End-to-End Entanglement

Once an entanglement between adjacent nodes is obtained, remote entanglement between non-adjacent nodes can be generated by performing entanglement swapping at intermediate nodes through atomic BSM.

By denoting with  $\tau^a$  and  $\nu^a$  the duration and the efficiency of a single atomic BSM, respectively, we derive in Lemma 2 the average time for an end-to-end entanglement generation  $T_{\mathcal{R}_{i,j}}$ .

**Lemma 2. (End-to-End Entanglement Generation Time)** *The expected time required to generate a remote entanglement between two non-adjacent nodes  $v_i$  and  $v_j$  through route  $\mathcal{R}_{i,j}$  is given by:*

$$T_{\mathcal{R}_{i,j}} = T_{\mathcal{R}_{\sigma_1, \sigma_n}} \quad (9)$$

with  $T_{\mathcal{R}_{\sigma_l, \sigma_m}}$  for the arbitrary sub-route  $\mathcal{R}_{\sigma_l, \sigma_m}$  recursively defined as in (10) shown at the top of next page, and with  $T_{\mathcal{R}_{\sigma_l, \sigma_m}}^c = \sum_{l=1}^{m-1} \tau_{\sigma_l, \sigma_{l+1}}^c$ .

*Proof: See Appendix C.* ■

From Lemma 2, the main result follows.

**Theorem 2. (End-to-End Entanglement Generation Rate)** *The expected entanglement generation rate  $R_{\mathcal{R}_{i,j}}(T^{ch})$  between nodes  $v_i$  and  $v_j$  through route  $\mathcal{R}_{i,j}$  is given in (11) shown at the top of next page, with  $T^{ch}$  denoting the quantum memory coherence time, and  $\tau_{\mathcal{R}_{\sigma_l, \sigma_m}}$  recursively defined as in (12) shown at the top of next page.*

*Proof: See Appendix D.* ■

**Remark.**  $\tau_{\mathcal{R}_{\sigma_l, \sigma_m}}$  given in (12) denotes the minimum storing time required to the quantum memories for the successful generation of an end-to-end entanglement.

## C. Discussion

Here we conduct a brief discussion stemming from the results derived through the paper.

The implicit assumption of our theoretical analysis is that the local entanglements start simultaneously, i.e., the swapping strategy is not optimized with respect to times  $T_{ij}$ . As instance, let us consider the route  $\{e_{1,2}, e_{2,3}, e_{3,4}\}$ , with  $T_{1,2}^s = {}^s T_{2,3} >> T_{3,4}^s$ . By neglecting the decoherence effects, it is equivalent to either: i) swapping first at  $v_2$  between link entanglements  $(v_1, v_2)$  and  $(v_2, v_3)$ , and then swapping at  $v_3$  between remote entanglements  $(v_1, v_3)$  and link entanglement  $(v_2, v_3)$ ; ii) swapping first at  $v_3$ , and then swapping at  $v_2$ . Differently, if we aim at minimizing the decoherence effects, it would be better to adopt the former strategy and to delay the link entanglement generation at  $e_{3,4}$  as much as possible. We leave the analysis of the swapping strategy optimization as a future work.

Furthermore, we explicitly neglect the effects of entanglement purification in our rate analysis. The rationale for this choice is that the adopted quantum repeater architecture is characterized by an extremely high fidelity, with values close to  $F = 0.99$  [11], [16]. Nevertheless, we plan to

$$T_{\mathcal{R}_{\sigma_l, \sigma_m}} = \begin{cases} \frac{\max \{T_{\mathcal{R}_{\sigma_l, \sigma_k}}, T_{\mathcal{R}_{\sigma_k, \sigma_m}}\} + \tau^a + \max \{T_{\mathcal{R}_{\sigma_l, \sigma_k}}^c, T_{\mathcal{R}_{\sigma_k, \sigma_m}}^c\}}{\nu^a}, & k = \left\lceil \frac{m+l}{2} \right\rceil & \text{if } m > l+1 \\ T_{\sigma_l, \sigma_{l+1}} & & \text{if } m = l+1 \end{cases} \quad (10)$$

$$R_{\mathcal{R}_{i,j}}(T^{\text{ch}}) = \begin{cases} 0 & \text{if } T^{\text{ch}} < \tau_{\mathcal{R}_{i,j}} - \min_{l=1, n-1} \{T_{\sigma_l, \sigma_{l+1}}^s - \tau_{\sigma_l, \sigma_{l+1}}\} \\ 1/T_{\mathcal{R}_{i,j}} & \text{otherwise} \end{cases} \quad (11)$$

$$\tau_{\mathcal{R}_{\sigma_l, \sigma_m}} = \begin{cases} \max \{\tau_{\mathcal{R}_{\sigma_l, \sigma_k}}, \tau_{\mathcal{R}_{\sigma_k, \sigma_m}}\} + \tau^a + \max \{T_{\mathcal{R}_{\sigma_l, \sigma_k}}^c, T_{\mathcal{R}_{\sigma_k, \sigma_m}}^c\}, & k = \left\lceil \frac{m+l}{2} \right\rceil & \text{if } m > l+1 \\ T_{\sigma_l, \sigma_{l+1}}^s & & \text{otherwise} \end{cases} \quad (12)$$

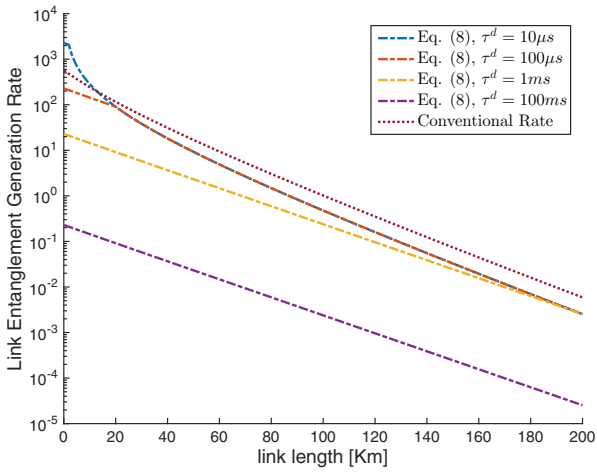


Fig. 3. Expected Link Entanglement Generation Rate  $R_{i,j}(T^{\text{ch}})$  between adjacent nodes  $v_i$  and  $v_j$  as a function of the optical link length  $d_{i,j}$  for different values of the time  $\tau^d$  required for atom cooling. Decoherence time  $T^{\text{ch}}$  equal to  $10\text{ms}$ . Logarithmic scale for  $y$  axis.

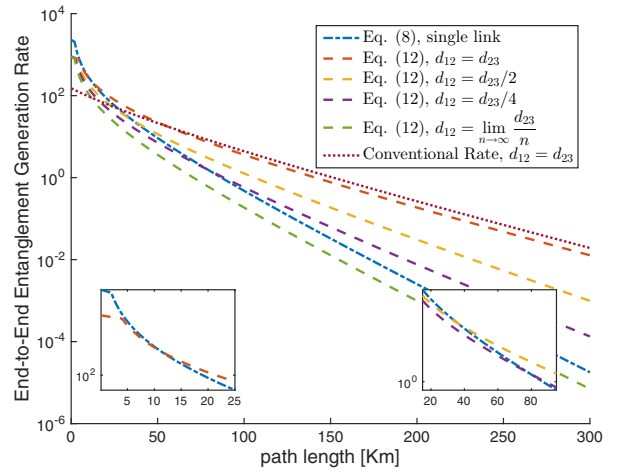


Fig. 4. Expected End-to-End Entanglement Generation Rate  $R_{\mathcal{R}_{1,3}}(T^{\text{ch}})$  between nodes  $v_1$  and  $v_3$  through route  $\mathcal{R}_{1,3} = \{e_{1,2}, e_{2,3}\}$  as a function of the total path length  $d_{1,2} + d_{2,3}$  for different values of  $d_{1,2}$ . Atom cooling time  $\tau^d$  and decoherence time  $T^{\text{ch}}$  equal to  $100\mu\text{s}$  and  $10\text{ms}$ , respectively. Logarithmic scale for  $y$  axis.

incorporate the purification mechanism within the end-to-end entanglement rate analysis in a future work.

#### IV. NUMERICAL RESULTS

Here, we evaluate both the link and the end-to-end entanglement rate by adopting the quantum repeater model shown in Fig. 2.

All the parameters have been set in agreement with experimental results [11], [13], but we note that the analytical results derived in Sec. III continue to hold for any different parameter setting. Specifically, we set  $p^{ht} = 0.53$ ,  $\nu^h = \nu^t = 0.8$ ,  $\nu^o = 0.390$ ,  $L_0 = 22\text{km}$ ,  $c_f = 2 * 10^8\text{m/s}$ ,  $\tau^p = 5.9\mu\text{s}$ ,  $\tau_h = 20\mu\text{s}$ ,  $\tau_t = 10\mu\text{s}$  and  $\tau^d = 100\mu\text{s}$ . Furthermore, we set  $\tau_{ij}^c = d_{i,j}/(2c_f)$  by neglecting the delay introduced by the optical amplifier, and we set  $\tau_o = \tau_a = 10\mu\text{s}$  analogously<sup>5</sup> to  $\tau_t$ . Finally, we reasonably assume quantum memories with

<sup>5</sup>The analytical results derived in Sec. III continue to hold for any different time-parameters setting.

coherence time  $T^{\text{ch}} = 10\text{ms}$ , since coherence times greater by more than an order of ten seconds have been already reported for the adopted qubit implementation (i.e.,  $^{87}\text{Rb}$ ) [17] and storage times exceeding  $10^{-5}\text{s}$  have been already reported for the atom-photon entanglement [16].

In Fig. 3, we show the expected link entanglement rate  $R_{i,j}(T^{\text{ch}})$  between adjacent nodes  $v_i$  and  $v_j$  given in (8) as a function of the optical link length  $d_{ij}$  for different values of the time  $\tau^d$  required for atom cooling (ranging from  $10\mu\text{s}$  to  $0.1\text{s}$ ). For performance comparison, we consider the approximation of the link entanglement rate recently proposed in [11], referred to as *Conventional Rate* and approximating the rate as  $(d_{ij}/c_f + \tau)/p_{ij}$  with  $\tau = 100\mu\text{s}$  and  $\nu^o = 1$  (i.e., ideal optical BSM). First, we note that the approximation slightly differs from the exact closed-form expression derived in (8) when  $\tau^o = \tau$ . Furthermore, we note that: i) the duty cycle duration significantly degrades the achievable rates for

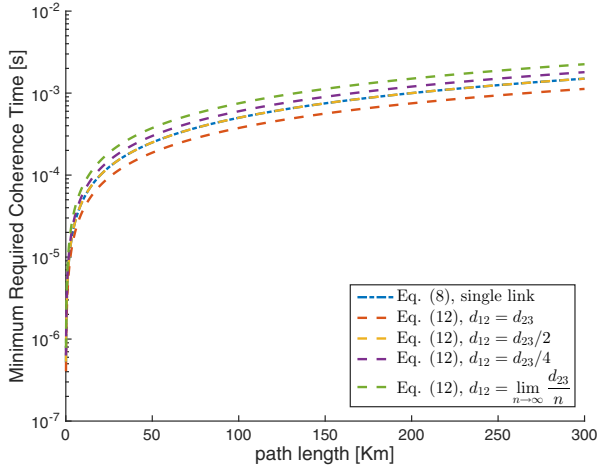


Fig. 5. Minimum Coherence Time  $\tau_{\mathcal{R}_{\sigma_1, \sigma_m}}$  required for an end-to-end entanglement between nodes  $v_1$  and  $v_5$  through route  $\mathcal{R}_{1,3} = \{e_{1,2}, e_{2,3}, e_{3,4}, e_{4,5}\}$  as a function of the total path length  $\sum_{i=1}^4 d_{i,i+1}$  for different values of  $d_{1,2}$ , with  $d_{2,3} = d_{3,4} = d_{4,5}$ . Atom cooling time  $\tau^d$  equal to  $100\mu s$ . Logarithmic scale for  $y$  axis.

shorter links, whereas it has no effect on longer links; ii) the higher is  $\tau^d$ , the larger is the range of distances affected by the duty cycle. This is reasonable: whenever it results  $t_{i,j} > \tau^d$  (i.e., long links), equation (7) degenerates in  $T_{i,j} = T_{i,j}^s / p_{i,j}$ .

In Fig. 4, we show the expected end-end entanglement rate  $R_{\mathcal{R}_{1,3}}(T^{\text{ch}})$  between nodes  $v_1$  and  $v_3$  through route  $\mathcal{R}_{1,3} = \{e_{1,2}, e_{2,3}\}$  given in (11) as a function of the total path length  $d_{1,2} + d_{2,3}$ . We consider four different topologies, by varying the ratio between the link lengths, plus an additional topology where there exists a direct link between  $v_1$  and  $v_3$  with length  $d_{1,3} = d_{1,2} + d_{2,3}$ . For performance comparison, we consider also the approximation of the end-to-end entanglement rate recently proposed in [11], referred to as *Conventional Rate*. We first note that approximation significantly differs from the exact closed-form expression derived in (8) whenever  $d_{1,2} \neq d_{2,3}$ , especially for longer links where the rate is over-estimated by roughly two order of magnitudes. Furthermore, we note that the exact closed-form expression derived in (8) is able to account for the rich dynamic imposed by the ratio of the link lengths. As an example, at  $d = 200\text{km}$ , the end-to-end entanglement rate can vary from 0.19 entanglements/second for  $d_{2,3} = d_{1,2}$  to 0.007 entanglements/second for  $d_{2,3} = 4d_{1,2}$ .

The rightmost box shows the presence of a critical path length value so that: i) for paths shorter than such a threshold, connecting  $v_1$  and  $v_3$  with a single link (i.e., without a repeater) with total length equal to  $d_{1,2} + d_{2,3}$  assures the highest entanglement rate: ii) on the contrary, for paths longer than such a threshold, connecting  $v_1$  and  $v_3$  through a repeater at  $v_2$  with  $d_{1,2} = d_{2,3}$  assures the highest entanglement rate. Clearly, this threshold effect is critical for selecting the shortest-path in complex networks, and it must be carefully taken into account. Similarly, the leftmost box shows the

presence of a critical path length value even when the repeater is not positioned in the path median.

Finally, in Fig. 5, we report the minimum coherence time  $\tau_{\mathcal{R}_{\sigma_1, \sigma_m}}$  required to the quantum memories for the successful generation of an end-to-end entanglement between nodes  $v_1$  and  $v_3$  through route  $\mathcal{R}_{1,3} = \{e_{1,2}, e_{2,3}\}$  as a function of the total path length  $d_{1,2} + d_{2,3}$ . The analytical expression of  $\tau_{\mathcal{R}_{\sigma_1, \sigma_m}}$  is given in (12). We first observe that the minimum coherence times are obtained by using a repeater positioned in the path median. Furthermore, quantum memories with coherence times exceeding the order of ten milliseconds can guarantee an end-to-end entanglement even for the larger values of considered path lengths.

## V. CONCLUSIONS

In this paper, we analytically derived the *end-to-end entanglement rate* between a couple of nodes through an arbitrary path. To this aim, we first modeled the entanglement generation through a stochastic framework that allowed us to jointly account for all the key physical-mechanisms affecting the end-to-end entanglement rate, such as decoherence time, atom-photon and photon-photon entanglement generation, entanglement swapping and imperfect bell-state measurement. Then, we derived the closed-form expression of the *end-to-end entanglement rate* for an arbitrary path, by relaxing the usual constraint that the repeaters must split the long-range link into segments of equal length. This is a valuable property, since it allows our rate expression to be used as routing metric by an arbitrary quantum routing protocol.

## APPENDIX

### A. Proof of Lemma 1

The thesis follows, after some algebraic manipulations, from the notable relations  $\sum_{n=0}^{\infty} nx^n = x/(x-1)^2$  and  $\sum_{n=0}^{\infty} x^n = 1/(1-x)$  for  $|x| < 1$ .

### B. Proof of Theorem 1

The thesis follows from (5) and Lemma 1, by noting that:

- i) the degradation of the qubit stored at each adjacent node starts at the emission of the telecom-wavelength photon during the local entanglement operation;
- ii) every time a link entanglement operation fails, a heralded local entanglement is re-generated at both  $v_i$  and  $v_j$ ;
- iii) given that at time  $T_{i,j}$  a link entanglement is generated, the most recent emission of telecom-wavelength photons happened at time  $T_{i,j} - \tau_{i,j}$ , independently from the number of failed link entanglement operations.

### C. Proof of Lemma 2

We prove the thesis through mathematical induction.

*Basis:* Show that the statement hold for when  $N = 1$  swapping rounds are required, i.e., when we have a route composed by at most two links. We set  $\mathcal{R}_{i,j} = \mathcal{R}_{13} = (e_{12}, e_{23})$  for the sake of notation simplicity.

To generate a remote entanglement between  $v_1$  and  $v_3$ , we need first to generate two link entanglements through  $e_{12}$

and  $e_{23}$ . This operation requires an average time equal to  $\max\{T_{12}, T_{23}\}$ . Once done, we have two cases.

- i) With probability  $\nu^a$  an entanglement swapping is generated at node  $v_2$ , and the swapping operation requires a time equal to  $\tau^a$ . Furthermore, an additional time equal to  $\max\{T_{12}^c, T_{23}^c\}$  is required for acknowledging  $v_1$  and  $v_3$  that a remote entanglement has been successfully generated through classical communication.
- ii) With probability  $\bar{\nu}^a \triangleq 1 - \nu^a$ , the swapping fails in a time equal to  $\tau^a$ . Furthermore, every time a BSM fails, the link entanglements through  $e_{12}$  and  $e_{23}$  must be re-generated. Hence, an additional time equal to  $\max\{T_{12}^c, T_{23}^c\}$  is required for informing  $v_1$  and  $v_3$  to start a new link entanglement generation process.

Hence, by denoting with  $T_{22} = \max\{T_{12}, T_{23}\} + \tau^a + \max\{T_{12}^c, T_{23}^c\}$  and by accounting for the notable relations  $\sum_{n=0}^{\infty} nx^n = x/(x-1)^2$  and  $\sum_{n=0}^{\infty} x^n = 1/(1-x)$  for  $|x| < 1$ , we obtain:

$$T_{13} = \sum_{k=0}^{\infty} (k+1)T_{22}(\bar{\nu}^a)^k \nu^a = \frac{T_{22}}{\nu^a} \quad (13)$$

and the statement is true for  $N = 1$ .

*Inductive Step:* Show that (10) holds for  $N + 1$  swapping rounds, given that (10) is true for  $N$  swapping rounds. We set  $\mathcal{R}_{i,j} = \mathcal{R}_{1,n} = (e_{1,2}, \dots, e_{n-1,n})$  with  $n = 2^{N+1}$  for the sake of notation simplicity.

To generate an end-to-end entanglement between  $v_1$  and  $v_n$ , we need first to generate two end-to-end entanglements between  $v_1, v_k$  and  $v_k, v_n$  with  $k = \lceil \frac{n+1}{2} \rceil$ , and this requires an average time equal to  $\max\{T_{\mathcal{R}_{1,k}}, T_{\mathcal{R}_{k,n}}\}$ . Then, we have two cases.

- i) With probability  $\nu^a$  an entanglement swapping is generated at node  $v_k$  in a time equal to  $\tau^a$ , and  $v_1$  and  $v_n$  become aware about the end-to-end entanglement generation through classical communication after an additional time equal to  $\max\{T_{\mathcal{R}_{1,k}}^c, T_{\mathcal{R}_{k,n}}^c\}$ .
- ii) With probability  $\bar{\nu}^a$ , the swapping fails in a time equal to  $\tau^a$ , and an additional time equal to  $\max\{T_{1k}^c, T_{k,n}^c\}$  is required to inform each node belonging to the route  $\mathcal{R}_{1,n}$  that the link entanglements must be re-generated.

Hence, by accounting for the notable relations  $\sum_{n=0}^{\infty} nx^n = x/(x-1)^2$  and  $\sum_{n=0}^{\infty} x^n = 1/(1-x)$  for  $|x| < 1$ , the thesis follows.

### D. Proof of Theorem 2

First, we note that:

- i) the degradation of the qubit stored at each adjacent node starts at the emission of the telecom-wavelength photon during the local entanglement operation;
- ii) every time an entanglement swapping operation fails, a link entanglement is re-generated at each edge  $e_{\sigma_i, \sigma_{i+1}} \in \mathcal{R}_{i,j}$  composing the route
- iii) given that at time  $T_{\mathcal{R}_{i,j}}$  an end-to-end entanglement is generated, the most recent round of link entanglement operations started at time  $T_{\mathcal{R}_{i,j}} - \tau_{\mathcal{R}_{i,j}}$  (with  $\tau_{\mathcal{R}_{i,j}}$  derived

in (12) by accounting for Lemma 2), independently from the number of failed link entanglement rounds;

- iv) given that at time  $T_{\mathcal{R}_{i,j}} - \tau_{\mathcal{R}_{i,j}}$  the most recent round of link entanglement operations started, the subsequent emission of telecom-wavelength photons for link  $e_{\sigma_i, \sigma_{i+1}}$  happened at time  $T_{\mathcal{R}_{i,j}} - \tau_{\mathcal{R}_{i,j}} + (T_{\sigma_i, \sigma_{i+1}}^s - \tau_{\sigma_i, \sigma_{i+1}})$ .

### REFERENCES

- [1] Q.-C. Sun, Y.-L. Mao, S.-J. Chen *et al.*, “Quantum teleportation with independent sources and prior entanglement distribution over a network,” *Nature Photonics*, vol. 10, no. 10, pp. 671–675, October 2016.
- [2] J. Yin, Y. Cao, Y.-H. Li *et al.*, “Satellite-based entanglement distribution over 1200 kilometers,” *Science*, vol. 356, no. 6343, pp. 1140–1144, 2017.
- [3] H.-J. Briegel, W. Dür, J. I. Cirac, and P. Zoller, “Quantum repeaters: The role of imperfect local operations in quantum communication,” *Physical Review Letters*, vol. 81, pp. 5932–5935, Dec 1998.
- [4] W. Dür, H.-J. Briegel, J. I. Cirac, and P. Zoller, “Quantum repeaters based on entanglement purification,” *Physical Review A*, vol. 59, pp. 169–181, Jan 1999.
- [5] M. Żukowski, A. Zeilinger, M. A. Horne, and A. K. Ekert, “‘‘event-ready-detectors’’ bell experiment via entanglement swapping,” *Physical Review Letters*, vol. 71, pp. 4287–4290, Dec 1993.
- [6] D. Deutsch, A. Ekert, R. Jozsa *et al.*, “Quantum privacy amplification and the security of quantum cryptography over noisy channels,” *Physical Review Letters*, vol. 77, pp. 2818–2821, Sep 1996.
- [7] T. Bacinoglu, B. Gulbahar, and O. B. Akan, “Constant fidelity entanglement flow in quantum communication networks,” in *GLOBECOM: the IEEE Global Telecommunications Conference*, Dec 2010, pp. 1–5.
- [8] R. Van Meter, T. Satoh, T. D. Ladd *et al.*, “Path selection for quantum repeater networks,” *Networking Science*, vol. 3, no. 1, pp. 82–95, Dec 2013.
- [9] S. Bratzik, S. Abruzzo, H. Kampermann, and D. Bruß, “Quantum repeaters and quantum key distribution: The impact of entanglement distillation on the secret key rate,” *Physical Review A*, vol. 87, p. 062335, Jun 2013.
- [10] N. K. Bernardes, L. Praxmeyer, and P. van Loock, “Rate analysis for a hybrid quantum repeater,” *Phys. Rev. A*, vol. 83, p. 012323, Jan 2011.
- [11] M. Uphoff, M. Brekenfeld, G. Rempe *et al.*, “An integrated quantum repeater at telecom wavelength with single atoms in optical fiber cavities,” *Applied Physics B*, vol. 122, no. 3, p. 46, Mar 2016.
- [12] A. G. Radnaev, Y. O. Dudin, R. Zhao, H. H. Jen, S. D. Jenkins, A. Kuzmich, and T. A. B. Kennedy, “A quantum memory with telecom-wavelength conversion,” *Nature Physics*, vol. 6, no. 11, pp. 894–899, 11 2010.
- [13] J. Hofmann, M. Krug, N. Ortegel *et al.*, “Heralded entanglement between widely separated atoms,” *Science*, vol. 337, no. 6090, pp. 72–75, 2012.
- [14] S. Ritter, C. Nilleke, C. Hahn *et al.*, “An elementary quantum network of single atoms in optical cavities,” *Nature*, vol. 484, no. 7393, pp. 195–200, 2012.
- [15] J. Borregaard, P. Kómár, E. M. Kessler *et al.*, “Long-distance entanglement distribution using individual atoms in optical cavities,” *Physical Review A*, vol. 92, p. 012307, Jul 2015.
- [16] C. Simon, M. Afzelius, J. Appel *et al.*, “Quantum memories,” *The European Physical Journal D*, vol. 58, no. 1, pp. 1–22, May 2010.
- [17] C. Deutsch, F. Ramirez-Martinez, C. Lacroûte *et al.*, “Spin self-rephasing and very long coherence times in a trapped atomic ensemble,” *Physical Review Letters*, vol. 105, p. 020401, Jul 2010.